Journal of Membrane Science 594 (2020) 117434

Contents lists available at ScienceDirect

Journal of Membrane Science

journal homepage: www.elsevier.com/locate/memsci

Effective removal of fluorescent microparticles as *Cryptosporidium parvum* surrogates in drinking water treatment by metallic membrane

Weiying Li[a,b,*], Wanqi Qi[c], Jiping Chen[c], Wei Zhou[c], Yue Li[c], Yiran Sun[c], Kai Ding[d]

[a] State Key Laboratory of Pollution Control and Resource Reuse, Tongji University, Shanghai, 200092, China
[b] Key Laboratory of Yangtze Aquatic Environment, Ministry of Education College of Environmental Science and Engineering, Tongji University, Shanghai, 200092, China
[c] College of Environmental Science and Engineering, Tongji University, Shanghai, 200092, China
[d] WPG (Shanghai) Smart Water Public Co., Ltd, China

ARTICLE INFO

Keywords:
Sintered metallic membrane
Cryptosporidium parvum
Fluorescent tracers
Drinking water treatment
Membrane fouling

ABSTRACT

The diarrhoea-causing parasitic protozoan *Cryptosporidium parvum* (*C. parvum*) cannot be efficiently removed by conventional drinking water treatment and poses a biological threat to public health. To ensure the biological safety, three kinds of metallic membranes, laminating metal mesh filter, non-woven metal filter and sintered metal fiber filter were employed to compare their properties. The results showed that the sintered membrane possessed the best filtration performance and lowest membrane resistance among three metallic membranes. Therefore, the sintered membrane was selected for subsequent experiments. Due to the low infectious dose of *C. parvum* and sophisticated detection methods, fluorescent particle tracers, Crypto-tracer-1, were chosen as a feasible surrogate was proposed to investigate the removal efficiency of sintered membrane for *C. parvum*. The results indicated that the tracer log removal value (LRV) ranged between 5.1 and 5.4 log10 under different filtration flux, which equivalently means that *C. parvum* could be completely removed and further tests are needed to confirm the results obtained using *C. parvum*. Furthermore, a pilot-scale study was performed for 10 weeks in full-scale drinking water treatment systems. The turbidity could be efficiently removed (outlet water of membrane was 0.08 ± 0.04 NTU) and the average transmembrane pressure recovery rate was 84.6% after physical backwash. Fouling mechanism analysis indicated that the interaction energy between foulants and membrane material became stronger over time. The practical operation results showed that sintered membrane performed well in continuous operation for a long time and also had a good anti-pollution ability. These findings could facilitate application of metallic membrane in drinking water treatment.

1. Introduction

Water quantity and quality underpin global development and sustainability. It is well known that the most of the raw waters in the world were polluted by pathogenic microorganisms, like *Salmonella*, *Vitriol cholera*, *Cryptosporidium parvum* (*C. parvum*) and so on [1]. The drinking water were threatened by biological contamination widely. A dramatic illustration of this effect was the outbreak occurred in Milwaukee, Wisconsin during the spring of 1993. Unfortunately, approximately 400,000 people were infected even though the utility met the requirements of the Safe Drinking Water Act [2]. And it has been generally recognized that *C. parvum* is a key significant diarrhoea-causing parasitic protozoan found both in humans and animals. Ensuring water security is a serious challenge from human health to the techno-economics of energy production [3]. Meanwhile *C. parvum* is so difficult to be inactivated with conventional treatment system [4–6], the United States Environmental Protection Agency (US EPA) has promulgated the Interim Enhanced Surface Water Treatment Rule to control the concentration of *C. parvum* in drinking water for the first time. In China, the new standards for drinking water quality (GB5749-2006) has been fully implemented since July 1, 2007, in which both *Giardia* and *C. parvum* are not allowed to be detected. As for the water treatment processes, the Safe Drinking Water Act (SDWA) Amendments of USA has forced water treatment professionals to consider the non-conventional treatment processes, such as membrane technologies, which would be capable of meeting the anticipated standards [7]. As an advanced process compared with conventional processes (e.g., coagulation, sedimentation, sand-filtration and chlorine disinfection), membrane technologies, such as Ultrafiltration (UF) and Microfiltration (MF), have been demonstrated to be a very efficient process to meet the requirements for pathogens (such as *Giardia* and *C. parvum*), turbidity, and virus removal through their physical removal characteristic. The potential range of

* Corresponding author. College of Environmental Science and Engineering, Tongji University, 1239, Siping Road, Shanghai, PR China.
E-mail address: liweiying@tongji.edu.cn (W. Li).

https://doi.org/10.1016/j.memsci.2019.117434
Received 9 April 2019; Received in revised form 24 July 2019; Accepted 29 August 2019
Available online 05 September 2019
0376-7388/

applications for membrane as well as research concerning various systems processes in water and wastewater treatment become more important and are spread all around the world [8].

Recently, some microplastics (MPs) were being detected in the treated water even through there were no MPs in the raw water [9]. Some MPs contamination may be produced in the water treatment processes and this might be verified by the material compositions of detected MPs that correspond to the polymer types used in the supply chain, such as the polymer membrane material. The organic membrane has the disadvantage of weak structure, temperature limited and is prone to denature and be contaminated, resulting in a shorter service life [10]. Although the organic membrane is cheaper than inorganic membrane, such as metallic membrane, it can be speculated that the organic membrane material may have the potential risk of leaking MPs into the water in long term operation. As one of the inorganic membrane, the metallic membranes were researched initially in 1979 [11]. Due to differences in manufacturing materials and processes, the main advantages of metallic membranes over organic ones are long term durability, strong structural integrity, high thermal stability (> 200 degree centigrade) and chemical stability in wide pH [12–14]. In general, metallic membranes favor applications under harsh temperature and chemical conditions, whereas organic membrane has the advantages of being economical and mass produced [10]. In comparison with the conventional another microfiltration membrane (manufactured by organic material and ceramic) with the same pore diameter, the metallic membranes show tighter pore size distribution and higher porosity, which guarantees that particles will not move into the filter material and the membrane have a lower resistance itself. Due to the aforementioned advantages as well as gradual reduction in cost, the metallic membranes open up new fields for applications in many different industries, such as chemical industry, laboratory technology, medical technology and drinking water treatment technology.

Previous researches have applied metallic membrane to component separation and acquired preferably effect. T.J. Phelps et al. [15] used a mixture of fluorescent polystyrene microspheres ranging in size from 0.5 to 6 μm in diameter simulated microorganisms in metallic membrane filtration studies and found that the membrane with 0.6 μm pore size could efficiently remove those small particles. Soo Hoon Choi et al. [16] used fluorescent particles with diameters of 0.5–0.7 μm to test the integrity of microfiltration membranes with nominal pore sizes of 0.25 μm. They found that the outflow mass of fluorescent particles depend linearly on the size of damage of membrane. Ree-Ho Kim et al. [17] used a metallic membrane for efficient and safe utilization of rainwater, and reported that metallic membranes were suitable to clarify rainwater because of their high removal rate of microorganisms and particulates. M.E. Aalami-Aleagha et al. [18] applied a prepared metallic layer as a perm selective film for filtration of glucose solution. The result certificated that the water flux was appropriate, and the prepared membrane was able to remove glucose from water efficiently. However, early studies of metallic membrane focused on gas separation and wastewater treatment other than drinking water and long-term research was not available. Therefore, it is necessary to explore the pathogenic microorganism and micro-particle removal characteristic of metallic membrane in drinking water treatment as well as the performance of the metallic membrane in long-term drinking water treatment process.

Because of the low infectious dose of *C. parvum*, extremely sensitive detection methods are required for water and food industries analysis [19], of which process would takes a long time. Thus, a series fluorescent particle tracers were selected instead of the direct use of *C. parvum* for more convenient and time-efficient analysis. Details will be provided in section 2.2.

In this study, filtration characteristics of three different metallic membranes (aminating metal mesh filter, non-woven metal filter and sintered metal fiber filter) with same pore size 0.3 μm were detected. These three metallic membranes were mad through three different manufacturing processes and by both stainless steel materials. The sintered one has an asymmetric structure, meanwhile the other two have symmetrical structures. These three different metallic membranes were studied to explore the influence of different manufacturing processes on the filtration performance for metallic membranes. Then the sintered metal filters was chosen from these metallic membranes for its good filtration performance and applied in the bench-scale experiment with the purpose of removal of *C. parvum* in drinking water In order to explore more about the sintered metal fiber performance in full-scale drinking water treatment systems, a pilot-scale study was continuously monitored for 10 weeks at a drinking water treatment plant in east China. These findings presented here would facilitate application of metallic membrane, providing more membrane material's selection for drinking water treatment.

Table 1
The Specification of metallic membrane.

Index	Laminating metal mesh filter	Non-woven metal filter	sintered metal filter
Membrane	Fuji FP-0.3	Fuji FA-0.3	SIKA-R0.3AS
Figure index	outer diameterϕ25 × effective length 500 mm/per unit		
Mode	Pressurized from outer		
Number of unit	2 units		
Membrane area	0.08 m^2 (0.04 m^2/per unit)		
Materials	SUS316	SUS316L	SUS316
Thickness	1.66 mm	1.66 mm	2–3 mm
Pore diameter	0.3 μm	0.3 μm	0.3 μm
Manufacturer	Fuji Filter MGF.CO.,LTD.	Fuji Filter MGF.CO.,LTD.	Germany GKN sinter GmbH CO.,LTD.

2. Experimental methods

2.1. Membrane module

The specification and the appearance of three metallic membranes, Laminating, Non-woven and Sintered metal filters, are summarized in Table 1.

2.2. The micro-particle removal characteristic experiment

The flow diagram of the micro-particle removal by three different metallic membranes in the dead-end flow mode was shown in Fig. 1a. The experiments were operated at the drinking water treatment plant and the sintered metal fiber filter was selected as a model of membrane by varying the water flow. The finished water of drinking water treatment plant was filtered by nanofiltration in order to avoid the interference and influence of the particulate matter. And the treated water was applied as experimental water for the microparticle removal characteristic experiment of sintered membrane. The system was operated with the various Tohcello PM series tracers with different diameter produced by the Toshin Kagaku CO., LTD. The dispersion tracers own the spherical shape and were made of bridging polymethacrylic acid methyl polymers. In all cases, diameters of micro-particle tracers ranged from 0.8 ~ to 6.6 μm. Three sorts of PM series tracers and Crypto-tracer-1 are added in the experimental water mentioned above. Especially, the Crypto-tracer-1 has the similar size of *C. parvum* and can be easily distinguished due to its fluorescence. Further characteristics are presented in Table 2. The Crypto - tracer - 1 was made of polymethyl methacrylate and provided by Toshin Chemical Industry Co., Ltd.

Apart from the micro-particle tracers introduced above, the *Microcystis aeruginosa* (*M. aeruginosa*, FACHB-192), which was purchased from the Freshwater Algae Culture Collection at the Institute of Hydrobiology, Chinese Academy of Sciences, was also used to test the characteristic of metallic membrane filtration as a kind of living and

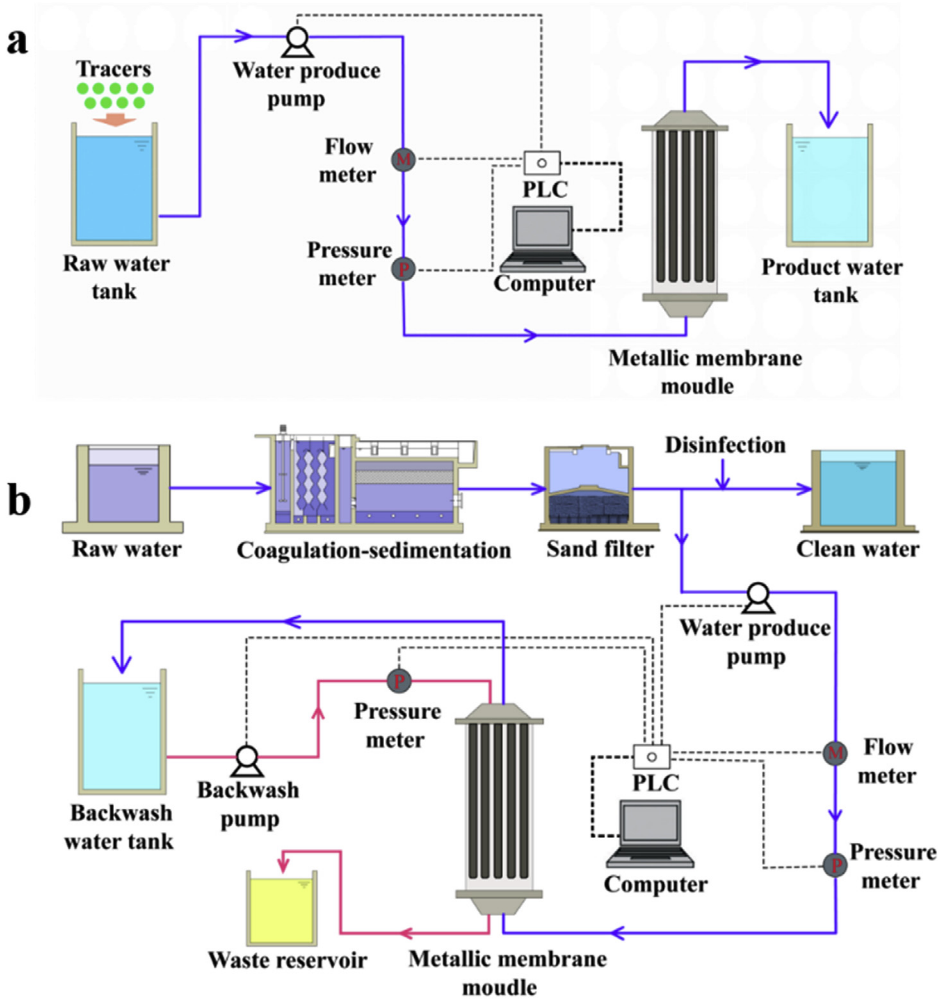

Fig. 1. The flow diagram of (a) metallic membrane filtration system, (b) pilot test at the drinking water treatment plant.

Table 2
The specifications of micro-tracers and *C. parvum*.

Index	PM-3KTAV	PM-4KTAV	PM-5KTAV	Crypto-tracer-1	*M. aeruginosa*	*C. parvum*
Average particle size (μm)	1.2	2.0	3.2	5.0	3.8	5.0
Gravity (g/cm^3)	1.18	1.18	1.18	1.19	1.08–1.14	1.05–1.10
Variation index (%)	6.6	6.6	7.0	19.7	–	–
Mesh (%)	12.9	16.1	20.7	8.8	–	–
Materials	Polymethyl methacrylate			Polymethyl acrylate	–	–

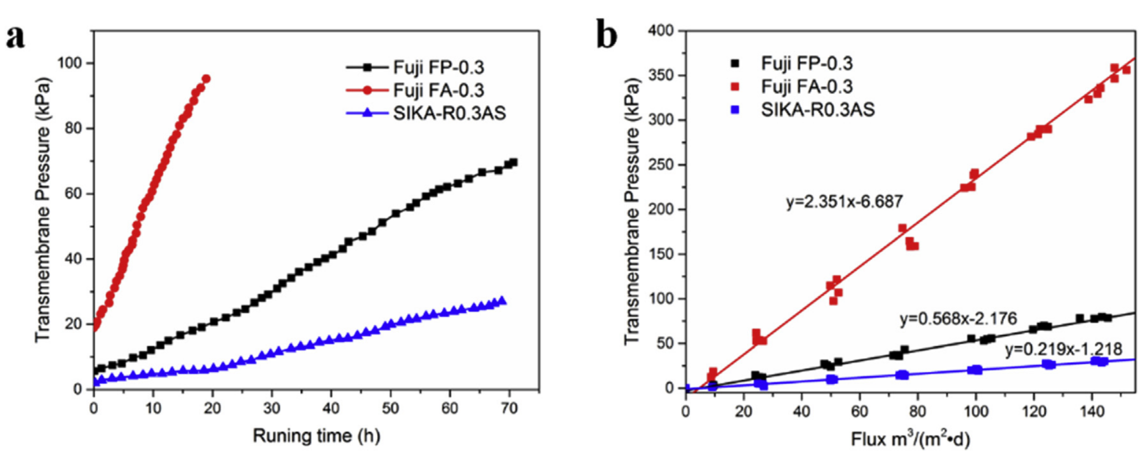

Fig. 2. The transmembrane pressure change of three membranes (a) under 150 m^3/(m^2·d) flux treating raw water, (b) under different pure water flux.

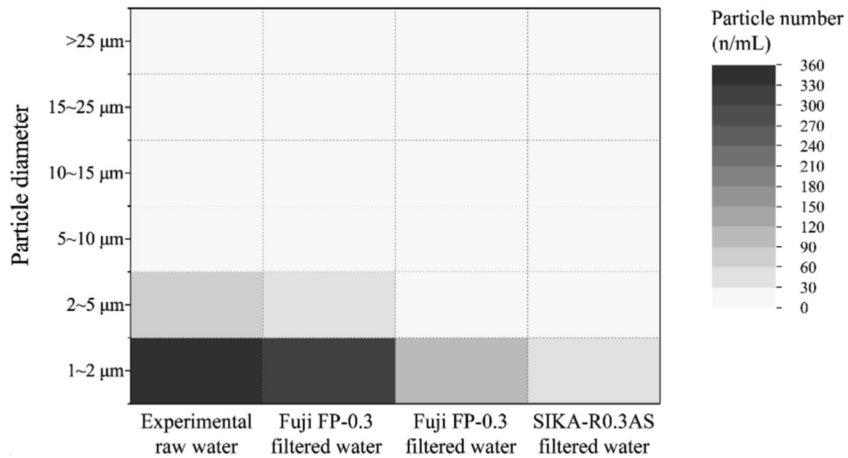

Fig. 3. Particles distribution of raw water and three different metallic membrane filtered water.

Table 3
The removal efficiency of micro-particles tracers and *M. aeruginosa* by sintered metallic membrane under different filtration rate.

Tracers (average diameter)	Flux ($m^3/m^2{\cdot}d$)	Numbers of particles(count/L)		Removal efficiency	
		Raw water	Membrane filtrate	(%)	LRV
PM-3KTAV (1.2 µm)	89	4.55E+10	3.59E+07	99.9212	3.104
	48		1.17E+07	99.9742	3.588
	25		1.38E+06	99.9970	4.518
PM-4KTAV (2.0 µm)	82	1.76E+10	6.23E+05	99.9965	4.451
	47		1.07E+06	99.9939	4.216
	24		3.53E+05	99.9980	4.697
PM-5KTAV (3.2 µm)	117	6.21E+09	2.27E+04	99.9996	5.438
	97		1.69E+04	99.9997	5.566
	67		8.91E+03	99.9999	5.844
	50		4.23E+03	99.9999	6.167
Crypto-tracer-1(5 µm)	133	4.25E+08	4.06E+03	99.9990	5.148
	100		2.01E+03	99.9995	5.325
	52		1.52E+03	99.9996	5.445
M. aeruginosa (3.8 µm)	86	9.33E+09	6.36E+06	99.9318	3.166
	45		7.04E+05	99.9925	4.122
	27		6.23E+05	99.9933	4.175

biological tracer. The BG-11 medium was employed to provide sufficient nutrients for algal growth of the *M. aeruginosa*, which is maintained in a growth chamber at 25 °C all day, with a 14 : 10 h light-dark regime under an illumination of 5000 lx [20]. When *M. aeruginosa* achieved the stationary phase (harvested at 28d), the harvested algae suspension was centrifuged at 10000g and 4 °C for 30 min. The algal cells remaining both in the centrifuge tubes and on the filters were collected and re-suspended with simulated water composed of 0.5 mM $CaCl_2$, 1.0 mM $NaHCO_3$, and 15.0 mM $NaClO_4$ in Milli-Q water. Subsequent experiments used this formula to dilute algae cells into experimental raw water according to the density requirement of experiment.

2.3. The characteristics evaluation

In this study, the pilot tests were carried out at a drinking water treatment plant in east China. The flux of metallic membrane filtration system was controlled in the range of 50–150 m/d. The raw water was filtered through convention treatment system and pressurized by a feeding pump to the membrane module. The membrane module contained 19 membrane elements and water was filtrated from the inside channel of lumens to the outside of the element during filtration process. All of the modules were set vertically and the raw water was fed from the bottom side of the module, as shown in Fig. 1b. The turbidity, total organic carbon (TOC) of membrane inlet and outlet water as well as the transmembrane pressure of the membrane were investigated.

2.4. Sampling and measurements

For the selection of a metallic membrane, TOC and micro-particles counter were detected by TOC4100 (Shimadzu, Japan), and MLC-7P micro-particle counter, respectively. This micro-particle counter has 6 channels (1–2 µm, 2–5 µm, 5–10 µm, 10–15 µm, 15–25 µm, 25 µm~). The turbidity was detected by the portable turbidity meter (2100Q, HACH, USA). The particularity of tracer was supplied by SEM (JMS-5310LV, produced by Shimadzu Corporation).

The total cells count (TCC) of *M. aeruginosa* were performed by flow cytometry [21,22]. Briefly, SYBR®-Green (Life) was diluted in dimethyl sulphoxide (DMSO) at the ration of 1:100. Samples of 500 µl was collected, stained with 5 µL diluted SYBR®-Green (Life) and stained incubated in the dark for 15 min at room temperature. Subsequently, cells were counted on a FACSCalibur flow cytometer (BD). Results were expressed in cells per milliliter (cells/mL).

2.5. Membrane fouling assessment

2.5.1. Interaction energy measurement

During the long-term operation test, the interaction energy per unit area between foulants and metallic membrane was calculated based on XDLVO theory [23]. Contact angles of ultrapure water, ethylene glycol and diiodomethane were measured with the method.

In an aquatic environmental system, the adhesion free energy between a membrane and foulant is the sum of the Lifshitz-van der Waals (LW), and Lewis acid–base interactions (AB), electrostatic double layer (EL) [24], because the effect of EL could be ignored in terms of the composition of the adhesion free energy [25], the interaction energy $\Delta G_{fwm}^{\mathrm{TOT}}$ in this paper was described in Eq. (1).

$$\Delta G_{fwm}^{\mathrm{TOT}} = \Delta G_{fwm}^{\mathrm{LW}} + \Delta G_{fwm}^{\mathrm{AB}} \tag{1}$$

f, m, w in the subscript represent the foulants, membrane and the water, respectively.

$\Delta G_{fwm}^{\mathrm{LW}}$ and $\Delta G_{fwm}^{\mathrm{AB}}$ can be calculated as follows [26,27]:

$$\Delta G_{fwm}^{LW} = \left(\sqrt{\gamma_w^{LW}} - \sqrt{\gamma_m^{LW}}\right)\left(\sqrt{\gamma_f^{LW}} - \sqrt{\gamma_w^{LW}}\right) \tag{2}$$

$$\Delta G_{fwm}^{AB} = 2\sqrt{\gamma_W^{+}}\left(\sqrt{\gamma_m^{-}} + \sqrt{\gamma_f^{-}} - \sqrt{\gamma_w^{-}}\right) + 2\sqrt{\gamma_w^{-}}\left(\sqrt{\gamma_m^{+}} + \sqrt{\gamma_f^{+}} - \sqrt{\gamma_w^{+}}\right)$$

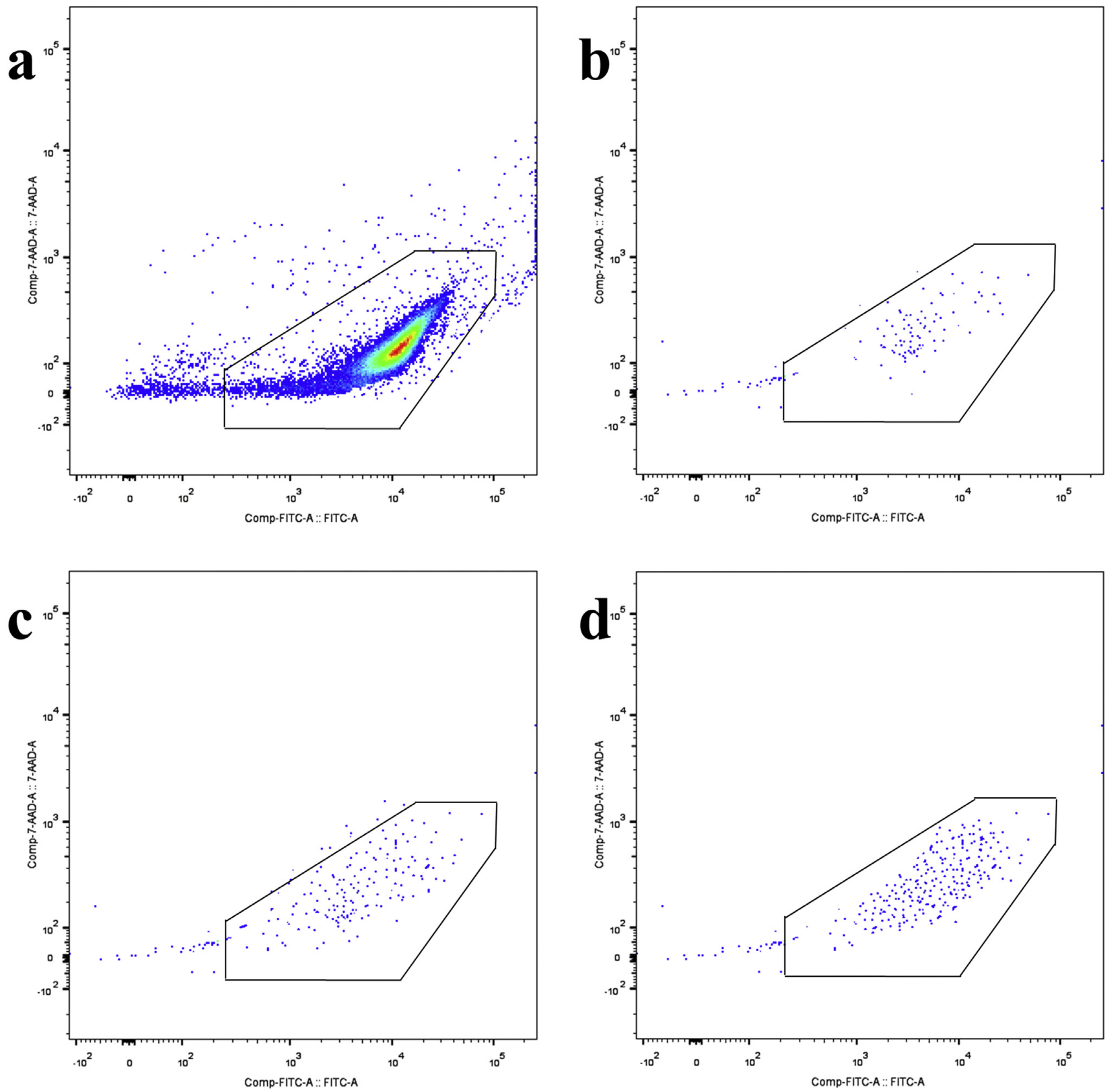

Fig. 4. The flow cytometry results of *M. aeruginosa* (a) in diluted 100 experimental water (described in section 2.2), (b) flux with 27 $m^3/m^2 \cdot d$ filtrated, (c) flux with 45 $m^3/m^2 \cdot d$ filtrated, (d) flux with 86 $m^3/m^2 \cdot d$ filtrated.

$$-2\left(\sqrt{\gamma_f^- \gamma_m^+} + \sqrt{\gamma_f^+ \gamma_m^-}\right) \tag{3}$$

Through a measurement of contact angle according to Young's equation [28] written as Eq. (4), the electron donating energy (γ^-), the electron-accepting energy (γ^+) and the LW component (γ^{LW}) can be obtained. The metallic membrane surface was treated as a solid for the purpose of attaining surface energy parameters.

$$(1+\cos\theta)\gamma_l^{TOT} = 2\left(\sqrt{\gamma_s^{LW}\gamma_l^{LW}} + \sqrt{\gamma_s^+\gamma_l^-} + \sqrt{\gamma_s^-\gamma_l^+}\right) \tag{4}$$

where the s in the subscript denotes the solid surface (metallic membrane or foulant), the l refers to the liquid used in each measurement, and the θ represents the contact angles, which were measured by an optical CA measuring instrument (OCA15EC, Dataphysics, Germany).

Before analysis, each virgin metallic membrane was pre-soaked in Milli-Q water for at least 12 h. All samples were dried at 40 °C in the oven for 48 h, and then the dried samples were measured at room temperature (25 °C) at least 10 times to acquire the average contact angle for each sample.

2.5.2. Membrane fouling resistance calculation

According to the Darcy filtration model and resistance-in-series model, membrane fouling can be can be expressed as [23,29]:

$$R_t = R_m + R_f = R_m + R_{ir} + R_{re} = \frac{\Delta P}{\mu J} \tag{5}$$

where R_t (m^{-1}), R_m (m^{-1}), R_f (m^{-1}), R_{ir} (m^{-1}), R_{re}(m^{-1}) are the total filtration resistance, intrinsic membrane resistance, total membrane fouling resistance, irreversible fouling resistance and reversible fouling resistance, respectively. ΔP (Pa) is the transmembrane pressure; the dynamic viscosity of permeate μ (Pa•s) depends on the liquid and temperature; J ($m^3/(m^2 \cdot s)$) is the permeate flux. In this study, the

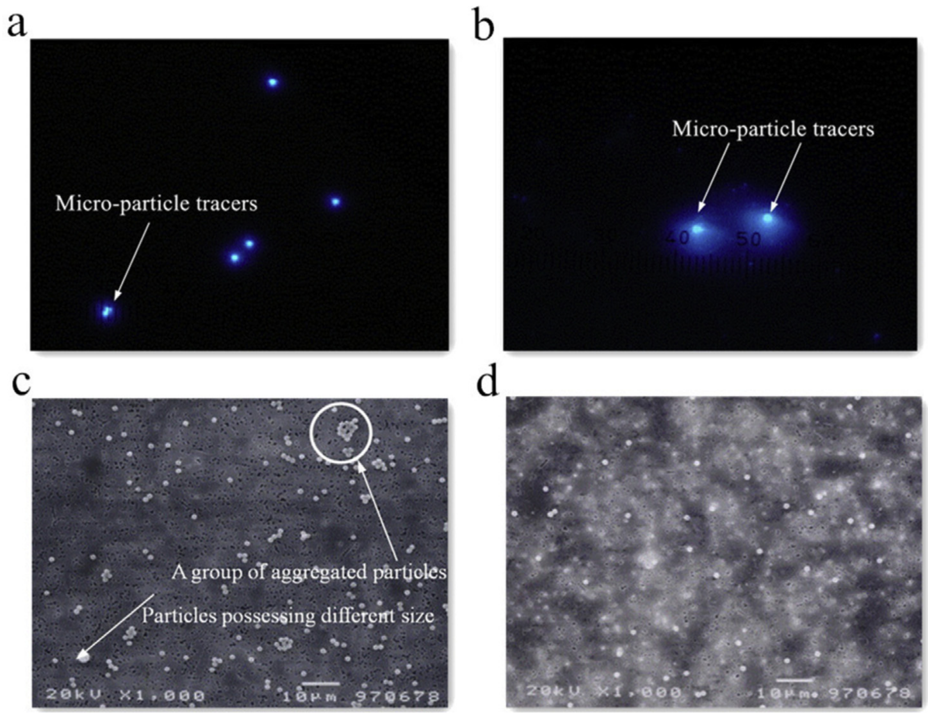

Fig. 5. Activated by UV fluorescence, (a) the micro-particle tracer (Crypto-tracer-1, 5 µm) in raw water (b) and in the sintered membrane filtrate effluent; (c) the distribution of micro-particles tracers (PM-3KTAV, 1.2 µm) in raw water, (d) in the sintered membrane filtrate effluent.

resistance that cannot be recovered by backwashing was called irreversible resistance. R_{ir} and R_{re} could be calculated by the following formulas:

$$R_{ir} = \frac{\Delta P_2}{\mu J} - R_m \tag{6}$$

$$R_{re} = \frac{\Delta P_1}{\mu J} - \frac{\Delta P_2}{\mu J} \tag{7}$$

whereΔP_1 is the experimental TMP data obtained at the end of filtration every filtration cycle, and ΔP_2 is the experimental TMP data obtained at the start of the next filtration cycle after hydraulic backwashing.

3. Results and discussion

3.1. The characteristics evaluation of three metallic membrane

In this part, the outlet water of the sand filter at the drinking water treatment plant was chosen as the experimental water and the device diagram was shown in Fig. 1b. Considering water-processing ability and economic factor, it is necessary to choose one kind of membrane with high flux. The transmembrane pressure change of three membranes under 150 $m^3/(m^2 \cdot d)$ flux was illustrated in Fig. 2a. Average filtration resistance increase rate over the operation time was introduced to evaluate membrane fouling. The average increase transmembrane pressure of the sintered metal fiber filter (SKIA-R0.3AS) was 0.36 kPa/d, which was the lowest among the three membrane modules. And the results of the other two membrane modules, laminating metal mesh filter (Fuji FP-0.3) and non-woven metal filter (Fuji FA-0.3) were 0.91 kPa/d and 4.03 kPa/d, respectively. Compared with organic or other inorganic membrane module, metallic membrane could run in the high flux (150 $m^3/(m^2 \cdot d)$, about several times of the average flux in the range between 2 and 2.5 m/d of previous membrane module) at a low or very same transmembrane pressure [30–33]. Apart from the well-known advantages of stainless steel filter, the sintered metal fiber filter took advantages in the self-supporting system, with the thickness of 2–3 mm while not causing a high pressure drop.

The results in Fig. 2b demonstrated the change of transmembrane pressure under different flux treating pure water. The transmembrane pressure increased accompanying with flux rising according to the linearity relationship. Besides, self-resistance of all three membranes can be obtained according to the Darcy filtration model as shown in equation (5). By substitution of the data, the membranes self-resistance *Rm* of SKIA-R0.3AS, Fuji FP-0.3 and Fuji FA-0.3 were $1.81 \times 10^{10} m^{-1}$, $4.67 \times 10^{10} m^{-1}$ and $2.04 \times 10^{11} m^{-1}$, respectively. The sintered one has an asymmetric structure, meanwhile the other two have symmetrical structures. Thus, the minimum membranes self-resistance of the sintered metal fiber filter resulted in the lowest resistance increase rate in Fig. 2a.

3.2. Performance of three metallic membrane in particle removal

The outlet water of the drinking water treatment plant was selected as the experimental raw water. Both the particle distributions of the raw water and filtered water from three types of metallic membrane module were detected and shown in Fig. 3.

As shown in the above figure, the numbers of particles of tap water were found around 95% in the range of 1 µm–5 µm in the experimental raw water and none was more than 25 µm. The numbers of the particles in the filtrates of non-woven metal filter and sintered metal filter ~~is~~ were both around 50–100 count/ml. The laminating metal mesh filter was found to be poor of particles removal, and the particles could only be removed at the level of 300 count/ml by this laminating membrane. Among the three metallic membranes, the sintered metal fiber filter was proved to be the best membranes for removing the particles at the level of 50–60 count/ml, indicating that thickness and the method to make metal filter dominated the efficiency of removing particles other than pore diameter. A large number of particles were in the range of 1–2 µm and there were less 10 count/ml in the range of 2–7 µm in filtrates.

The experimental raw water turbidity was 0.16 ± 0.05 NTU. Even so, it could be further reduced to 0.10 ± 0.04 NTU, 0.11 ± 0.05 NTU and 0.07 ± 0.03 NTU by filtrating with laminating metal mesh filter, non-woven metal filter and sintered metal fiber filter, respectively.

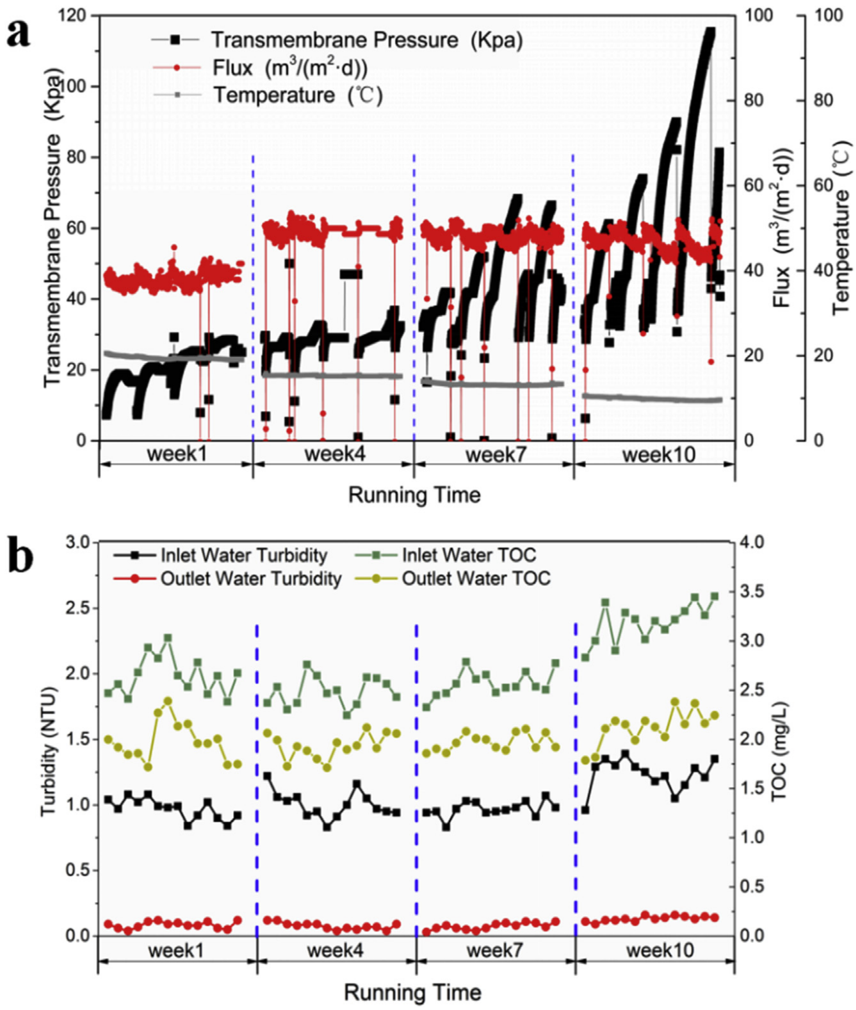

Fig. 6. During the 10 weeks operational period, (a) the variations in flux, TMP and temperature; (b) both inlet and outlet water quality of the sintered membrane model.

Table 4
Inlet and outlet water quality of sintered metallic membrane during the whole operation.

Water quality index	Inlet water	Outlet water
Turbidity (NTU)	0.92 ± 0.22	0.09 ± 0.04
TOC (mg/L)	2.675 ± 0.775	2.025 ± 0.313

Turbidity is a parameter used to reflect the content of suspended particles in water [34]. After running for a short time, filter cake layer accumulated on the surface. The layer served as a thin separative layer through mechanic sieving and intercepted most of the particles and colloid, which elucidated that metallic membrane has an outstanding removal capability of turbidity. The results depicted that the removing rate of three metallic membranes on water particulate matter (such as micro-particle and turbidity index) was obvious and the sintered metal membrane had a better performance compared to the other two. Therefore the sintered metal membrane was selected in the next bench-scale and pilot-scale tests.

3.3. The micro-particle removal characteristic experiment

The characteristic of particles removal was carried out at the drinking water treatment plant according to Fig. 1a. The raw water of experiment was by NF module to exclude interfere caused by other factors and adding the different PM series, Crypto-tracer-1 micro-particles and *M. aeruginosa*. The sintered membrane was employed as the membrane model. The raw water and sintered membrane filtrate were random sampled under different flux. The number of every sort of particles and cells in raw water of experiment were controlled at 10^8-10^{10} count/l. The results are shown in Table 3.

The data during the period were collected to evaluate the operation and cleaning of the metallic membrane plant at the drinking water treatment plant. The results shown in Table 3 indicated that all of micro-particles were removed efficiently by the sintered membrane when the flux ranged from 25 to 133 $m^3/(m^2 \cdot d)$.

The average removal efficiency of PM-5KTAV (3.2 μm), PM-4KTAV (2.0 μm) and PM-3KTAV (1.2 μm) is a 5log, 4log and 3log, respectively. Especially, the average removal efficiency of Crypto-tracer-1(5.0 μm) and *M. aeruginosa* (3.8 μm) was a 5log and 3 - 4log under different flux. The higher flux was selected, the lower removal efficiency was obtained. Because crypto-tracer-1 could be excited to luminescence by UV-Fluorescence, the number of particles is easy to be identified and counted under SEM. Fig. 5 provided the micro-particle tracers (crypto-tracer-1: 5 μm and PM-3KTAV: 1.2 μm) in raw water and in metallic membrane filtrate. As shown in Fig. 5c, some of the micro-particles tracers would like to aggregate together and possess a bigger size due to electrostatic attraction and hydrophobic action between the micro-particles; furthermore, it will be easier for the aggregated group to be filtered by sintered membrane. Under a higher flux, the micro-particles tracers are less likely to stick together due to the stronger hydraulic

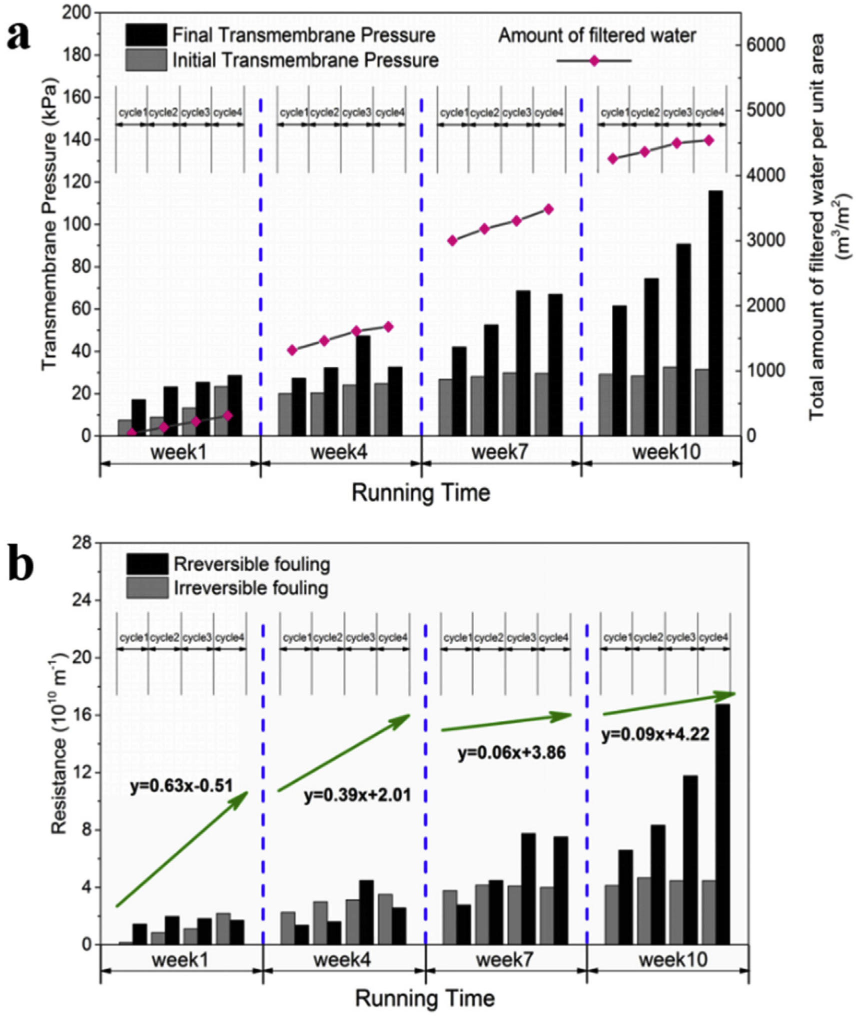

Fig. 7. During the operation, (a) initial and final transmembrane pressure after backwash and total amount of filtered water on per unit area; (b) reversible and irreversible fouling resistances of sintered membrane and linear fitting of irreversible resistances with operation cycles in every week.

Table 5
Average contact angles, surface tension parameters and interaction energy between membrane and foulant.

Sample name	Contact angle (°)			γ^{LW}	γ^{-}	γ^{+}	γ^{AB}	γ^{TOT}	ΔG_{fwm}^{LW}	ΔG_{fwm}^{AB}	ΔG_{fwm}^{TOT}
	θ_{wat}	θ_{eth}	θ_{dii}								
virgin sintered membrane	83.32	54.52	33.72	–	–	–	–	–	–	–	–
1st week's membrane	62.33	38.64	23.11	46.805	17.705	0.000	0.090	46.895	−8.322	−36.640	−44.962
4th week's membrane	59.18	34.88	19.33	47.977	19.835	0.001	0.282	48.258	−8.008	−39.253	−47.261
7th week's membrane	79.71	48.02	32.58	43.121	4.696	0.061	1.067	44.188	−6.990	−58.420	−65.410
10th week's membrane	83.55	61.24	43.36	37.880	6.073	0.022	0.727	38.608	−5.466	−56.019	−61.485

ΔG_{fwm} is the interaction energy between metallic membrane and foulant, mJ/m^2.

shear force, so that the removal efficiency was a little lower under a higher flux. The same phenomenon was found in the filtration of *M. aeruginosa* using sintered membrane (shown in Fig. 4 and Table 3). Different from the crypto-tracer and PM-tracer, the *M. aeruginosa* possess some special characteristics such as compressibility [35]. Moreover, algal debris may appear in water due to interference factors such as pump shear stress [36,37]. Therefore, the TMP would be higher and the shear stress would be stronger under a higher flux, which allows algal cells and debris to penetrate the membrane material and results in a lower removal efficiency. Due to the pore blockage of membrane and the formation of cake layer, the filtration capacity of the membrane might be enhanced and the membrane could get a better removal efficiency for microorganisms with smaller size [38].

3.4. Pilot test of sintered membrane filtration

The pilot tests were carried out at drinking water treatment plant in east China using sintered metal filter and the device diagram was shown in Fig. 1b. At the initial stage, the membrane filtration operated steadily, the transmembrane pressure was below 30 kPa and the membrane module had a certain practicality and durability (Fig. 6a). Due to the short interval, the transmembrane pressure could almost completely recover after back flush. However, when the running time was over 7 week, the transmembrane pressure was speeded up and the highest transmembrane pressure could reach 115.44 kPa, which was 6-fold compare to the initial transmembrane pressure.

The turbidity of inlet and outlet water during the whole operation were 0.92 ± 0.22 NTU and 0.09 ± 0.04 NTU, respectively (Fig. 6b). The average removal rate of turbidity was about 88.04%. During the three months operational period, the outlet water of sintered membrane remained steady was still under 0.13 NTU regardless of the running time and the change of inlet turbidity, which mean the sintered membrane had a good performance in turbidity removal. However, due to the pore size, the ability of sintered membrane to remove organic matter was limited. The average removal rate of organic matter was about 24.32% during the three months operational period and the outlet TOC was 2.025 ± 0.313 mg/L as shown in Table 4.

Fig. 7a described the initial and final transmembrane pressure variation in each filtration cycle. The final transmembrane pressure of metallic membrane module increased from 1.4-fold to 3.8-fold when the membrane run approximately 24 h, as expressed by the dark bars. A new filtration cycle begun after backwashing, and the newly initial transmembrane was marked using the light bars. The initial and final transmembrane pressure were compared after each physical backwash, Consequently, the average transmembrane pressure recovery rate was 84.6% and the transmembrane pressure increase of −3.7%–76%. The metallic membrane appeared the phenomenon that the recovery rate of backwashing decrease, while the transmembrane pressure increased rapidly. The increased transmembrane pressure corresponded to the part of hydraulically irreversible fouling and the physical cleaning of water backwashing cannot effectively recover the membrane flux, which means chemical cleaning should be applied.

The reason why the recovery rate of backwashing decreased was owing to the irreversible membrane fouling. The membrane pore and inner surface was clogged or adsorbed gradually by organic matter with running time, which reduced the pore diameter and caused the formation of irreversible fouling. It could be observed in Fig. 7b that the irreversible fouling apparently increased with operation cycles in the 1st week. After 4 weeks' operation, the slope of the linear fitting of irreversible resistance and operating cycles became less lower, which meant that the irreversible resistance's increment was not clear and irreversible fouling tended to be dynamically steady, meanwhile the reversible fouling resulted from the formation of cake layers.

According to XDLVO theory, the contact angles of virgin metallic membrane and the foulants after 1, 4, 7, and 10 weeks' operation respectively, were measured to calculate the adhesion free energies of the membranes and the foulants. As shown in Table 5, the contact angle of ultrapure water is correlated to the hydrophobicity of membrane material; specifically, the contact angle of the virgin metallic membrane was 83.32° and smaller than 90°, which meant a slight hydrophilicity of the membrane. It also can be found that the ultrapure contact angle of foulants increased with filtration. The higher water contact angle indicates the stronger membrane hydrophobicity [27]. The result indicated that the foulants adhering to the metallic membrane surface might possess hydrophobic tendencies after filtration operation. In Table 5, the adhesion free energies ΔG_{fwm}^{TOT} were negative values in different weeks, showing an attractive effect between foulant and metallic membrane [39,40]. A higher negative value of interaction energy indicates stronger effect. There was a tendency that the attractive interaction between foulants and metallic membrane became stronger over operation time and the foulants were more easily absorbed in the membrane pores or rapped on the membrane surfaces resulting in irreversible membrane fouling.

4. Conclusion

Possessing the characteristic of long life durability, high structural integrity and thermal stability, etc., three different metallic membranes were employed to compare their filtration properties. Due to having the best filtration performance and the lowest membrane resistance among the three metallic membranes, the sintered membrane was selected to explore the removal efficiency of *C. parvum* and evaluate the filtration capacity in real drinking water treatment.

In this study, a novel idea that fluorescent particle tracers were chosen as a feasible surrogate was proposed to investigate the removal efficiency of sintered membrane for *C. parvum*. The results indicated that the *C. parvum* could be completely removed by sintered membrane.

Additionally, the sintered membrane operated steadily in 10 weeks' operation. The average transmembrane pressure recovery rate was 84.6% after backwash. And there was a tendency that the attractive interaction between foulants and metallic membrane became stronger over operation time. The results indicated that the sintered membrane had a good performance on anti-pollution. These findings provided that the sintered membrane has wide application foreground in drinking water treatment.

Acknowledgments

We are grateful for the cooperation and participation of the utilities that were involved in this project, which is supported by National Key Technology R&D Program of Research on urban water system construction and safety assurance technology in Xiong an New Area of China (Project NO. 2018ZX07110-0082). We also thank for technical support by program of study on water quality safety evaluation and risk control under multi-source water supply in Qingdao city (Project NO. 20182766) with Qingdao Water Group Co. Ltd and research on water quality assurance and operation maintenance technology of secondary water supply system (Project NO. 20183231) with WPG (Shanghai) Smart Water Public Co., Ltd.

References

[1] Y. Jiang, P. Biswas, J.D. Fortner, A review of recent developments in graphene-enabled membranes for water treatment, Environ. Sci. Water Res. 2 (2016) 915–922.
[2] F. KR, L. DA, Milwaukee's crypto outbreak:investigation and recommendations, J. Am. Water Work. Assoc. 88 (9) (1996) 87–94.
[3] Y.Q. Guo, L.M. Bai, X.B. Tang, Q.J. Huang, B.H. Xie, T.Y. Wang, J.L. Wang, G.B. Li, H. Liang, Coupling continuous sand filtration to ultrafiltration for drinking water treatment: improved performance and membrane fouling control, J. Membr. Sci. 567 (2018) 18–27.
[4] P. Beaudeau, J. Schwartz, R. Levin, Drinking water quality. and hospital admissions of elderly people for gastrointestinal illness in Eastern Massachusetts, 1998-2008, Water Res. 52 (2014) 188–198.
[5] M.E. Warkiani, L.Q. Chen, C.P. Lou, H.B. Liu, R. Zhang, H.Q. Gong, Capturing and recovering of Cryptosporidium parvum oocysts with polymeric micro-fabricated filter, J. Membr. Sci. 369 (2011) 560–568.
[6] A. Zahedi, A. Gofton, T. Greay, P. Monis, C. Oskam, A. Ball, A. Bath, A. Watkinson, I. Robertson, U. Ryan, Profiling the diversity of Cryptosporidium species and genotypes in wastewater treatment plants in Australia using next generation sequencing, Sci. Total Environ. 644 (2018) 635–648.
[7] W. Gao, H. Liang, J. Ma, M. Han, Z.-l. Chen, Z.-s. Han, G.-b. Li, Membrane fouling control in ultrafiltration technology for drinking water production: a review, Desalination 272 (2011) 1–8.
[8] H.Q. Chang, H. Liang, F.S. Qu, B.C. Liu, H.R. Yu, X. Du, G.B. Li, S.A. Snyder, Hydraulic backwashing for low-pressure membranes in drinking water treatment: a review, J. Membr. Sci. 540 (2017) 362–380.
[9] K. Novotna, L. Cermakova, L. Pivokonska, T. Cajthaml, M. Pivokonsky, Microplastics in drinking water treatment - current knowledge and research needs, Sci. Total Environ. 667 (2019) 730–740.
[10] G.Q. Lu, J.C.D. da Costa, M. Duke, S. Giessler, R. Socolow, R.H. Williams, T. Kreutz, Inorganic membranes for hydrogen production and purification: a critical review and perspective, JCIS 314 (2007) 589–603.
[11] E.J. Dobo, T.E. Graham, Inorganic anisotropic hollow fiber, U.S. Patent 4 (1979) 153 175.
[12] S.-M. Lee, I.-H. Choi, S.-W. Myung, J.-y. Park, I.-C. Kim, W.-N. Kim, K.-H. Lee, Preparation and characterization of nickel hollow fiber membrane, Desalination 233 (2008) 32–39.
[13] B. Damit, B.L. Bischoff, T.J. Phelps, C.Y. Wu, M.D. Cheng, Filtration of bioaerosols using a granular metallic filter with micrometer-sized collectors, J. Environ. Eng. 140 (2014) 5.
[14] L.F. Han, Z.L. Xu, Y. Cao, Y.M. Wei, H.T. Xu, Preparation, characterization and permeation property of Al_2O_3, Al_2O_3-SiO_2 and Al_2O_3-kaolin hollow fiber membranes, J. Membr. Sci. 372 (2011) 154–164.
[15] T.J. Phelps, A.V. Palumbo, B.L. Bischoff, C.J. Miller, L.A. Fagan, M.S. McNeilly, R.R. Judkins, Micron-pore-sized metallic filter tube membranes for filtration of particulates and water purification, J. Microbiol. Methods 74 (2008) 10–16.
[16] S.H. Choi, J. Yang, C. Suh, J. Cho, Use of fluorescent silica particles for checking the integrity of microfiltration membranes, J. Membr. Sci. 367 (2011) 306–313.
[17] R.-H.K. a*, S.L. a, J.-O.K. b, Application of a metal membrane for rainwater

utilization: filtration characteristics and membrane fouling, Desalination 177 (2005) 121–132.
[18] M.E. Aalami-Aleagha, S.S. Madaeni, P. Daraei, A new application of thermal spray in preparation of metallic membrane for concentration of glucose solution, J. Therm. Spray Technol. 18 (2009) 519–524.
[19] C. Thiruppathiraja, S. Kamatchiammal, P. Adaikkappan, M. Alagar, An advanced dual labeled gold nanoparticles probe to detect Cryptosporidium parvum using rapid immuno-dot blot assay, Biosens. Bioelectron. 26 (2011) 4624–4627.
[20] B. Liu, H. Liang, F. Qu, H. Chang, S. Shao, N. Ren, G. Li, Comparison of evaluation methods for Microcystis cell breakage based on dissolved organic carbon release, potassium release and flow cytometry, Chem. Eng. J. 281 (2015) 174–182.
[21] J.L. Sun, L.J. Bu, L. Deng, Z. Shi, S.Q. Zhou, Removal of Microcystis aeruginosa by UV/chlorine process: inactivation mechanism and microcystins degradation, Chem. Eng. J. 349 (2018) 408–415.
[22] D. van der Kooij, H.R. Veenendaal, Regrowth Problems and Biological Stability Assessment in the Netherlands, (2014).
[23] Y. Tan, T. Lin, W. Chen, D. Zhou, Effect of organic molecular weight distribution on membrane fouling in an ultrafiltration system with ozone oxidation from the perspective of interaction energy, Environ. Sci. Water Res. 3 (2017) 1132–1142.
[24] Q.H. She, R. Wang, A.G. Fane, C.Y.Y. Tang, Membrane fouling in osmotically driven membrane processes: a review, J. Membr. Sci. 499 (2016) 201–233.
[25] A. Subramani, E.M.V. Hoek, Direct observation of initial microbial deposition onto reverse osmosis and nanofiltration membranes, J. Membr. Sci. 319 (2008) 111–125.
[26] C.Y.Y. Tang, T.H. Chong, A.G. Fane, Colloidal interactions and fouling of NF and RO membranes: a review, Adv. Colloid Interface Sci. 164 (2011) 126–143.
[27] W. Huang, H. Chu, B. Dong, J. Liu, Evaluation of different algogenic organic matters on the fouling of microfiltration membranes, Desalination 344 (2014) 329–338.
[28] F. Gao, J. Wang, H.W. Zhang, M.Q.A. Hang, Z. Cui, G. Yang, Interaction energy and competitive adsorption evaluation of different NOM fractions on aged membrane surfaces, J. Membr. Sci. 542 (2017) 195–207.
[29] T. Lin, Z.J. Lu, W. Chen, Interaction mechanisms of humic acid combined with calcium ions on membrane fouling at different conditions in an ultrafiltration system, Desalination 357 (2015) 26–35.
[30] P. Neuman, R. Röhlig, A. Kohstη, A. Semrau, Metallic membrane, Filtr. Sep. 35 (1) (1998) 40–42.
[31] S. Xia, Y. Zhou, R. Ma, Y. Xie, J. Chen, Ultrafiltration of humic acid and surface water with tubular ceramic membrane, Desalin. Water. Treat. 51 (2013) 5319–5326.
[32] T. Zsirai, P. Aerts, S. Judd, Reproducibility and applicability of the flux step test for a hollow fibre membrane bioreactor, Separ. Purif. Technol. 107 (2013) 144–149.
[33] D.J. Miller, S. Kasemset, D.R. Paul, B.D. Freeman, Comparison of membrane fouling at constant flux and constant transmembrane pressure conditions, J. Membr. Sci. 454 (2014) 505–515.
[34] R. Floris, G. Moser, K. Nijmeijer, E.R. Cornelissen, Effect of multicomponent fouling during microfiltration of natural surface waters containing nC(60) fullerene nanoparticles, Environ. Sci. Water Res. 3 (2017) 744–756.
[35] L.X. Pinho, J. Azevedo, A. Brito, A. Santos, P. Tamagnini, V.J.P. Vilar, V.M. Vasconcelos, R.A.R. Boaventura, Effect of TiO2 photocatalysis on the destruction of Microcystis aeruginosa cells and degradation of cyanotoxins microcystin-LR and cylindrospermopsin, Chem. Eng. J. 268 (2015) 144–152.
[36] B. Liu, F. Qu, H. Liang, Z. Gan, H. Yu, G. Li, B. Van der Bruggen, Algae-laden water treatment using ultrafiltration: individual and combined fouling effects of cells, debris, extracellular and intracellular organic matter, J. Membr. Sci. 528 (2017) 178–186.
[37] P. Rajasekhar, L. Fan, N. Thong, F.A. Roddick, A review of the use of sonication to control cyanobacterial blooms, Water Res. 46 (2012) 4319–4329.
[38] A. Ding, J.L. Wang, D.C. Lin, X.X. Cheng, H. Wang, L.M. Bai, N.Q. Ren, G.B. Li, H. Liang, Effect of PAC particle layer on the performance of gravity-driven membrane filtration (GDM) system during rainwater treatment, Environ. Sci. Water Res. 4 (2018) 48–57.
[39] T. Lin, B. Shen, W. Chen, X. Zhang, Interaction mechanisms associated with organic colloid fouling of ultrafiltration membrane in a drinking water treatment system, Desalination 332 (2014) 100–108.
[40] T. Lin, Z. Lu, W. Chen, Interaction mechanisms of humic acid combined with calcium ions on membrane fouling at different conditions in an ultrafiltration system, Desalination 357 (2015) 26–35.